

Optical Sensor for the Detection of Caspase-9 Activity in a Single Cell

Paul M. Kasili,[†] Joon Myong Song, and Tuan Vo-Dinh*

Contribution from the Advanced Biomedical Science and Technology Group, Life Sciences Division, Oak Ridge National Laboratory, P.O. Box 2008, Oak Ridge, Tennessee 37831-6101

Received July 18, 2003 E-mail: vodinh@ornl.gov

Abstract: We demonstrate for the first time, the application and utility of a unique optical sensor having a nanoprobe for monitoring the onset of the mitochondrial pathway of apoptosis in a single living cell by detecting enzymatic activities of caspase-9. Minimally invasive analysis of single live MCF-7 cells for caspase-9 activity is demonstrated using the optical sensor which employs a modification of an immunochemical assay format for the immobilization of nonfluorescent enzyme substrate, Leucine-GlutamicAcid-Histidine-AsparticAcid-7-amino-4-methylcoumarin (LEHD-AMC). LEHD-AMC covalently attached on the nanoprobe tip of an optical sensor is cleaved during apoptosis by caspase-9 generating free AMC. An evanescent field is used to excite cleaved AMC and the resulting fluorescence signal is detected. By quantitatively monitoring the changes in fluorescence signals, caspase-9 activity within a single living MCF-7 cell was detected. By comparing of the fluorescence signals from apoptotic cells induced by photodynamic treatment and nonapoptotic cells, we successfully detected caspase-9 activity, which indicates the onset of apoptosis in the cells.

Introduction

Minimally invasive analysis of cellular signaling pathways inside single live cells is becoming increasingly important fundamentally because cells in a population respond asynchronously to external stimuli.¹ There is a need to further our understanding of basic cellular signaling processes in order to yield new information that is not available from population-averaged cellular measurements. In addition, many cellular signaling pathways act on time scales of a few seconds and there is critical need for single-cell measurement techniques with similar time resolution. Not only is there a need to temporally resolve such measurements, there is also a need to spatially resolve them. For these reasons, continued progress in cellular physiology requires new measurement strategies, which can be applied to individual cells² with great temporal and spatial resolution. For this purpose, the optical sensor having a nanoprobe is a suitable technology with great potential for obtaining intracellular measurements of biological entities as will be demonstrated in this work.

Biosensors have played a key role in the development of minimally invasive, highly sensitive, and selective technologies for biochemical analysis.³ One of the most recent advances in

the field of biosensors has been the development of nanoscale size optical sensors capable of detecting and responding to the interaction between analytes of biomedical interest and their corresponding antibody within single live cells.^{4–6} Minimally invasive analysis of living cells involves penetrating individual live cells without causing physiological or biological damage with resultant biochemical consequences. Intracellular measurements are made possible by the nanoscale size of the optical nanosensor in comparison to the dimensions of the cell, typically 1–2 orders of magnitude. Optical sensors having nanoprobes are thus crucial for minimally invasive analysis because they allow the penetration and sampling of individual live cells in their physiological state without disrupting their normal functions, hence allowing the continuation of vital cellular processes such as mitosis.⁷ These antibody-based optical sensors rely on excitation using the evanescent field generated by total internal reflection at the nanotip of the optical nanosensor, thus exciting only molecules in close proximity to the boundary interface of the optical sensor nanotip. The evanescent field generated at

[†] E-mail address: kasilipm@ornl.gov.

- (1) Brasuel, M.; Kopelman, R.; Miller, T. J.; Tjalkens, R.; Philibert, M. A. Fluorescent nanosensors for intracellular chemical analysis: decyl methacrylate liquid polymer matrix and ion-exchange-based potassium PEBBLE sensors with real-time application to viable rat C6 glioma cells. *Anal. Chem.* **2001**, *73*(10), 2221–2228.
- (2) Luzzi, V.; Lee, C. L.; Allbritton, N. L. Localized sampling of cytoplasm from *Xenopus* oocytes for capillary electrophoresis. *Anal. Chem.* **1997**, *69*(23), 4761–4767.

- (3) Vo-Dinh, T.; Allain, L. Biosensors for Medical Applications. *CRC Handbook for Biomedical Photonics*; Vo-Dinh, T., Ed.; 2003, New York: CRC Press; p 31.
- (4) Cullum, B.; Griffin, G. D.; Miller, G. H.; Vo-Dinh, T. Intracellular measurements in mammary carcinoma cells using fiber-optic nanosensors. *Anal. Biochem.* **2000**, *277*(1), 25–32.
- (5) Kasili, P. M.; Cullum, B. M.; Griffin, G. D.; Vo-Dinh, T. Nanosensor for In-Vivo Measurement of the Carcinogen Benzo [a] Pyrene in a Single Cell. *J. Nanosci. Nanotechnol.* **2003**, *2*(6), p 653–658.
- (6) Vo-Dinh, T.; Alarie, J. P.; Cullum, B. M.; Griffin, G. D. Antibody-based nanoprobe for measurement of a fluorescent analyte in a single cell. *Nat. Biotechnol.* **2000**, *18*(7), 764–767.
- (7) Vo-Dinh, T. Nanobiosensors: Probing the Sanctuary of Individual Living cells. *J Cellular Biochem., Suppl.* **161** **2002**, 39, 154.

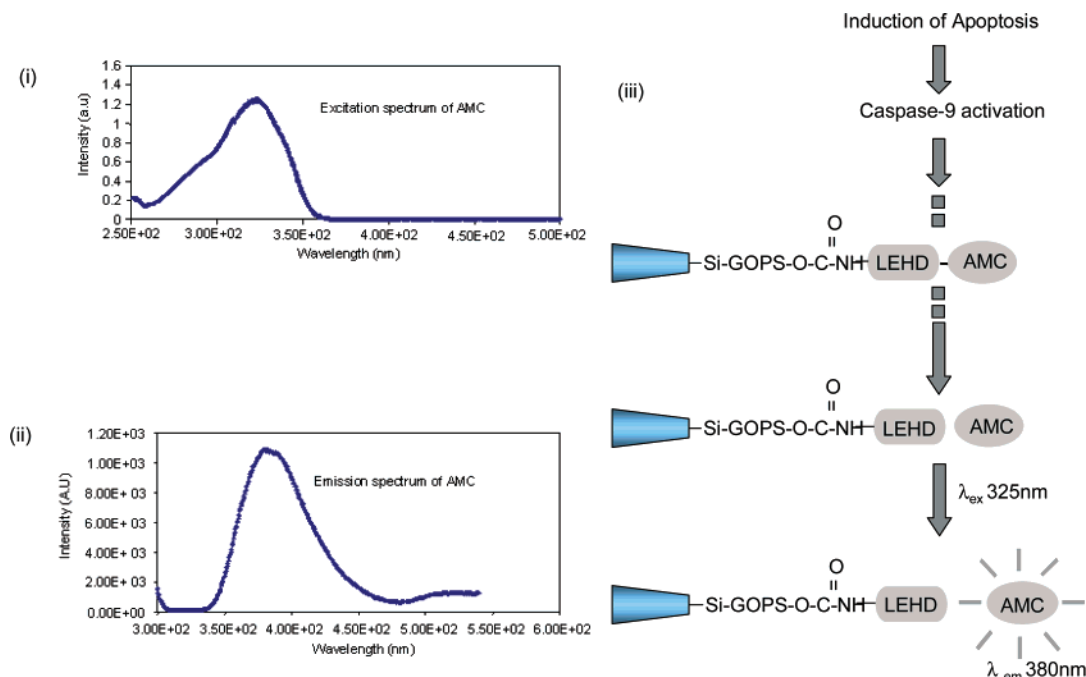


Figure 1. (i) Absorption spectrum of AMC (10^{-3} M). (ii) Emission spectrum of AMC (10^{-3} M). Excitation and emission spectra were acquired to determine where to excite and detect AMC. (iii) Diagrammatic representation of ALA induced apoptosis, involving the activation of caspase-9 followed by the cleavage of LEHD-AMC and subsequent detection of free AMC.

the nanotip of the optical sensor is a result of the sensor tip being smaller than the wavelength of the laser beam, leading to a diffraction-limited condition that does not allow photons from the laser beam to be transmitted through the tip of the nanoprobe but rather allows energy to be transmitted in the form of an interfacial leaky surface mode, which is propagated as the evanescent field exciting only molecules on the periphery of the tip.

We have developed a unique enzyme optical sensor based on an enzyme–substrate nanoprobe to detect and identify surface dependent cleavage events of caspase-9 in a single live MCF-7 cell. The modified assay format consists of a solid phase for the immobilization of caspase-9 substrate, Leucine-GlutamicAcid-Histidine-AsparticAcid-7-amino-4-methylcoumarin (LEHD-AMC), which consists of a tetrapeptide, LEHD, coupled to a fluorescent molecule, AMC. LEHD-AMC exists as a nonfluorescent substrate prior to cleavage by caspase-9, and after cleavage, free AMC fluoresces when excited at 325 nm (Figure 1 (iii)).

Figure 1(i),(ii) shows the excitation and emission spectra of AMC in PBS acquired using a Fluoromax-3 spectrofluorimeter (Jobin Yvon Inc., Edison, NJ). The excitation spectrum represents the relative ability of various wavelengths to stimulate AMC fluorescence emission, while the emission spectrum represents the relative fluorescence intensity when AMC is excited. In contrast to traditional, discontinuous, nonequilibrium ELISA-type cleavage assays that cannot accurately model dynamic binding mechanisms, the optical sensor permits investigation of surface cleavage phenomena, in addition to providing a simple way to detect caspase-9 in single cells. Caspase-9 is a prominent member of a family of death-specific enzymes known as cysteine-dependent aspartate-specific proteases, the caspases.⁸ Caspase-9 is activated via mitochondrial involvement in the apoptotic pathway. Cells exposed to apoptotic stimuli release cytochrome *c* from mitochondria into the

cytosol. In the cytosol, cytochrome *c* interacts with apoptotic protease activating factor-1 (Apaf-1).⁹ The cytochrome *c*/Apaf-1 complex cleaves the inactive caspase-9 proenzyme to generate active caspase-9 enzyme.¹⁰ Activated caspase-9 exhibits distinct substrate recognition properties and initiates the proteolytic activities of other downstream caspases, which degrade a variety of substrates, resulting in the systematic disintegration of the cell^{11–13} and, ultimately, cell death.

The enzyme substrate-based optical nanoprobe works on the same principle of evanescent field excitation by means of an exponentially decaying surface energy wave with a penetration depth that allows only AMC molecules in close proximity to the boundary interface of the optical nanoprobe tip to be excited and detected. This feature is important because it underlines the operating principle of the nanoprobe in the sense that only the cleaved AMC will be excited in the near field of the optical nanoprobe. An additional feature of the sensor is its selectivity. Selectivity is dependent upon the selective cleavage capabilities for specific sequences by caspase-9. Another advantage of the optical sensors' feature of excitation and detection in the evanescent field is the reduction of sources of background,

- (8) Mehmet, H. Apoptosis: Caspases find a new place to hide. *Nature* **2000**, *403*(6765), 29–30.
- (9) Liu, X.; Kim, C. N.; Yang, J.; Jemmerson, R.; Wang, X. Induction of apoptotic program in cell-free extracts: Requirement for dATP and Cytochrome *c*. *Cell* **1996**, *86*(1), 147–157.
- (10) Li, P.; Nijhawan, D.; Budihardjo, I.; Srinivasula, S. M.; Ahmad, M.; Alnemri, E. S.; Wang, X. Cytochrome *c* and dATP-Dependent Formation of Apaf-1/Caspase-9 Complex Initiates an Apoptotic Protease Cascade. *Cell* **1997**, *91*, 479–489.
- (11) Deveraux, Q. L.; Roy, N.; Stennicke, H. R.; Van Arsdale, T.; Zhou, Q.; Srinivasula, S. M.; Alnemri, E. S.; Salvesen, G. S.; Reed, J. C. IAPs block apoptotic events induced by caspase-8 and cytochrome *c* by direct inhibition of distinct caspases. *EMBO J.* **1998**, *17*(8), 2215–2223.
- (12) Sun, X.; MacFarlane, M.; Zhuang, J.; Wolf, B. B.; Green, D. R.; Cohen, G. M. Distinct caspase cascades are initiated in receptor-mediated and chemical-induced apoptosis. *J. Cell Biol.* **1999**, *274*(8), 5053–5060.
- (13) MacFarlane, M.; Cain, K.; Sun, X. M.; Alnemri, E. S.; Cohen, G. M. Processing/activation of at least four interleukin-1beta converting enzyme-like proteases occurs during the execution phase of apoptosis in human monocytic tumor cells. *J. Cell Biol.* **1997**, *137*(2), 469–479.

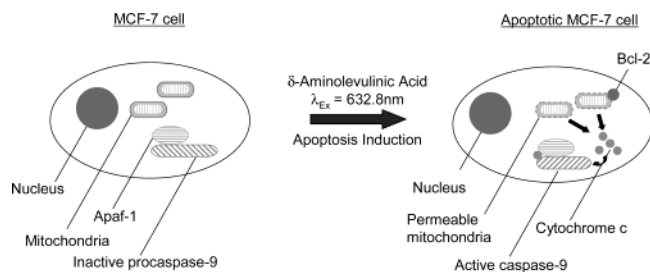


Figure 2. Diagrammatic representation of the ALA photoactivation process in a MCF-7 cell. On the left is representation of a MCF-7 cell prior to the induction of apoptosis and similarly on the right is a representation of a MCF-7 cell shortly after the induction of apoptosis showing the activation of caspase-9, ultimately leading to apoptosis.

particularly specular scattering, Rayleigh scattering, and Raman scattering from regions outside the near field. The optical sensors' mode of excitation and detection unlike other techniques for molecular detection does not compromise throughput and signal-to-noise ratio. Furthermore, due to its nanoscale size, the optical nanoprobe does not compromise the integrity of the cell when performing intracellular analysis. This has been illustrated in a previous study whereby a single cell was microscopically monitored after probing the cytoplasm of the cell with a nanoprobe of the optical sensor. The cell was observed and it was found that the cell carried out normal cellular activities, specifically mitosis.⁷

In this work, we demonstrate for the first time, the application and utility of an optical sensor having nanoprobe for the detection and identification of the onset of the mitochondrial pathway of apoptosis in a single live MCF-7 cell by detecting the enzymatic activity of caspase-9. To perform these measurements, we covalently immobilized caspase-9 substrate, LEHD-AMC, onto the tip of the nanofiber. Photodynamic therapy (PDT) protocols (Figure 2) employing δ -aminolevulinic acid (ALA) were used to induce apoptosis¹⁴ in MCF-7 cells. Briefly, caspase-9 is present in the cell after apoptosis has been induced. It typically exists in a proenzyme form procaspase-9, prior to apoptosis induction. MCF-7 cells exposed to apoptotic stimuli release cytochrome *c* from mitochondria into the cytosol. In the cytosol, cytochrome *c* interacts with apoptotic protease activating factor-1 (Apaf-1).⁹ The cytochrome *c*/Apaf-1 complex cleaves the inactive procaspase-9, a proenzyme to generate the active enzyme, caspase-9.¹⁰ Activated caspase-9 then initiates the proteolytic activities of other downstream caspases. These caspases degrade a variety of substrates, resulting in the systematic disintegration of the cell. Caspase-9 is capable of cleaving multiple LEHD-AMC substrates. This is a typical mechanism of action characteristic of enzymes, the ability to hydrolyze multiple substrates because they do not undergo change when they are involved in the cleavage reactions and they can therefore be applied to multiple substrates. Our measurement system consists of the tetrapeptide substrate Leucine-Glutamic Acid-Histidine-Aspartic Acid-7-amino-4-methoxycoumarin (LEHD-AMC), which is selectively cleaved by activated caspase-9. The principle of this system is the specific recognition of caspase-9 substrate LEHD-AMC and its subsequent processing and conversion to the corresponding products, LEHD and AMC. Since caspase-9 plays a central role

in the induction of apoptosis, tetrapeptide-based optical sensors are used to determine their role in response to ALA in MCF-7 cells. Caspase-9 protease activity was monitored after ALA-PDT induced apoptosis in MCF-7 cells by detecting the fluorescence emitted by AMC after caspase-9 recognizes and cleaves LEHD-AMC. The recognition of LEHD-AMC by caspase-9 is immediately followed by a cleavage reaction yielding the fluorescent AMC which is excited with a helium-cadmium (HeCd) laser to generate a measurable fluorescence signal.

This reaction accomplishes specific binding between the active site of caspase-9 and LEHD-AMC, conversion of the substrate to product, and release of the product LEHD and AMC from the active center, which in turn leads to the specific detection of intracellular caspase-9 activity. By comparing the fluorescence signal generated from AMC within cells with activated caspase-9 and from those with inactive caspase-9, we are able to successfully detect caspase-9 activity within a single living MCF-7 cell.

Materials and Methods

Chemicals and Reagents. δ -Aminolevulinic acid (ALA), phosphate buffered saline (PBS), hydrochloric acid (HCl), nitric acid (HNO₃), glycidyoxypropyltrimethoxysilane (GOPS), 1,1'-carbonyldiimidazole (CDI), and anhydrous acetonitrile were purchased from Sigma-Aldrich, St. Louis, MO. Caspase-9 substrate, LEHD-7-amino-4-methylcoumarin (AMC), 2x reaction buffer, dithiothreitol (DTT), and dimethyl sulfoxide (DMSO) were purchased from BD Biosciences, Palo Alto, CA.

Cell Lines. Human breast cancer cell line, MCF-7, was obtained from American Type Culture Collection (Rockville, MD, Cat-no. HTB22). MCF-7 cells were grown in Dulbecco's Modified Eagle's Medium (DMEM) (Mediatech, Inc., Herndon, VA) supplemented with 1 mM l-glutamine (Gibco, Grand Island, NY) and 10% fetal bovine serum (Gibco, Grand Island, NY). Baseline static culture productivity for each cell line was established in growth medium (described above) in standard T25 tissue culture flasks (Corning, Corning, NY). The flasks were incubated in a humidified incubator at 37 °C, 5% CO₂, and 86% humidity. Cell growth was monitored daily by microscopic observation until a 60–70% state of confluence was achieved. The growth conditions were chosen so that the cells would be in log phase growth during photosensitizer treatment with ALA but would not be so close to confluence that a confluent monolayer would form by the termination of the chemical exposure.¹⁵ In preparation for experiments, cells were harvested from the T25 flasks and 0.1-mL (10⁵ cells/mL) aliquots were seeded into 60-mm tissue culture dishes (Corning Costar Corp., Corning, NY) for overnight attachment. The MCF-7 cells were studied as four separate treatment groups with the first group being the experimental, exposed to 0.5 mM ALA for 3 h followed by photoactivation.¹⁶ This involved incubating the cells at 37 °C in 5% CO₂ for 3 h with 0.5 mM ALA. Following incubation the MCF-7 cells were exposed to red light from a HeNe laser (λ 632.8 nm, <15 mW, Melles Griot, Carlsbad, CA) positioned about 5.0 cm above the cells for 5 min at a fluence of 5.0 mJ/cm² to photoactivate ALA and subsequently induce apoptosis. The second group was the "treated control" and was exposed to 0.5 mM ALA for 3 h without photoactivation. The third group was the "untreated control" and was exposed to light from a HeNe laser positioned about 5.0 cm above the cells for 5 min at a fluence of 5.0 mJ/cm² without 0.5 mM ALA. The fourth group was the "untreated control",

(14) Hengartner, M. O. Apoptosis. DNA destroyers. *Nature* **2001**, *412*(6842), 27.

(15) Cullum, B.; Vo-Dinh, T. The development of optical nanosensors for biological measurements. *Trends Biotechnol.* **2000**, *18*(9), 388–393.

(16) Hilf, R.; Havens, J. J.; Gibson, S. L. Effect of Aminolevulinic Acid on Protoporphyrin IX Accumulation in Tumor Cells Transfected with Plasmids Containing Porphobilinogen Deaminase DNA. *Photochem. Photobiol.* **1999**, *70*(3), 334–340.

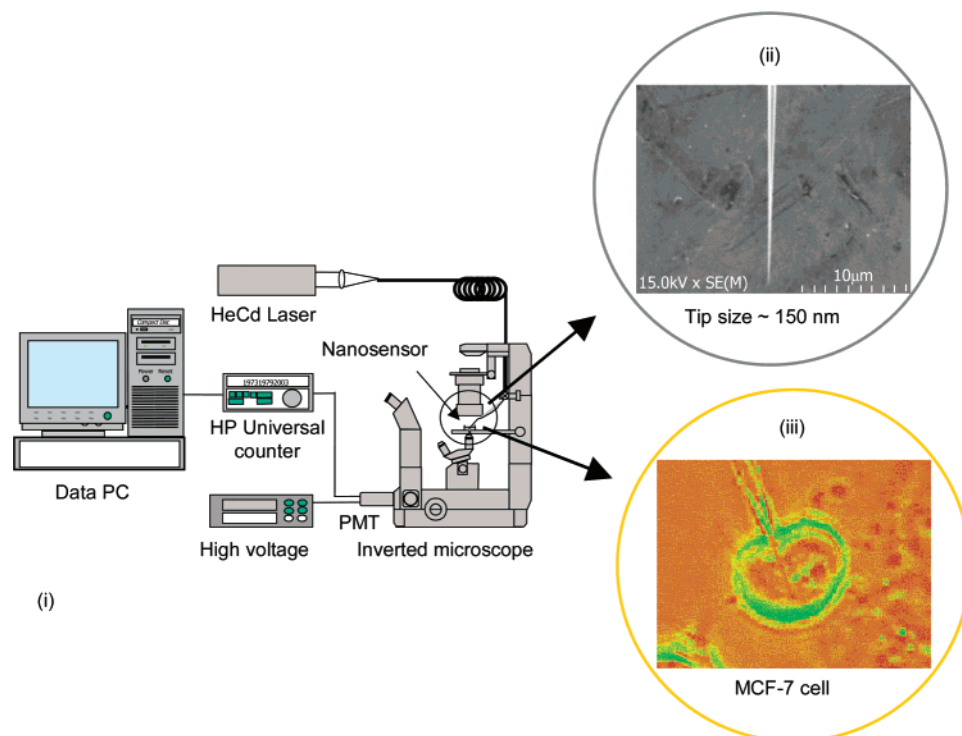


Figure 3. (i) Schematic diagram of fluorescence measurement system used for data acquisition and processing. (ii) Scanning electron micrograph of a nanotip after coating with 100 nm of silver metal, achieving a final tip diameter of 150 nm. (iii) Image of optical nanoprobe inserted into a single live MCF-7 cell. This image shows how we performed the intracellular measurements of MCF-7 cells.

which received neither ALA nor photoactivation. The percentage of MCF-7 cells undergoing apoptosis was analyzed. It should be noted that the percent of cells undergoing apoptosis is given as a relative number. This is because as a subpopulation of cells is undergoing apoptosis, another subpopulation is undergoing mitosis, therefore creating a dynamic baseline. The percent of cells undergoing apoptosis was calculated using dead cell count assay, and a static baseline of 1.75×10^6 cells was used. The group one MCF-7 cells, exposed to 0.5 mM ALA for 3 h followed by photoactivation, a total of 31.385% (± 0.1) cells underwent apoptosis. In the second group, the “treated control” exposed to 0.5 mM ALA for 3 h without photoactivation, a total dead cell count of 1.294% (± 0.1) was observed apoptosis. In the third group, the “treated control” exposed to photoactivation without 0.5 mM ALA, a total of dead cell count of 1.258% (± 0.1) was observed. In the fourth group, the “untreated control”, which received neither ALA nor photoactivation, a total dead cell count of 1.129% (± 0.1) was observed. ALA-PDT induced apoptosis was confirmed using Rhodamine 123 staining. Rhodamine 123 is a cell-permeant, cationic, fluorescent dye that is readily sequestered by active mitochondria in cells undergoing apoptosis without inducing cytotoxic effects¹⁷ and has been used in previous studies to view apoptosis.^{18,19}

Preparation of Enzyme Substrate-Based Optical Sensors Having Nanoprobe Tips. Preparation of enzyme substrate-based nanoprobes of the optical sensors involves cutting and polishing plastic clad silica (PCS) fibers with a 600- μm -diameter core (Fiberguide Industries, Stirling, NJ). The optical fibers were pulled to a final tip diameter of 50 nm using the current state-of-the-art in micropipet pulling technology, the P-2000 system (Sutter Instruments, Novato, CA), and then

coated with 100 nm of silver metal (99.999% pure) using a thermal evaporation deposition system (Cooke Vacuum Products, South Norwalk, CT) achieving a final diameter of 150 nm (Figure 3 (ii)). The nanotips were derivatized to allow the immobilization of enzyme substrate. Derivatization involved a multistep procedure. The fused silica optical fibers were acid-cleaned followed by several rinses with distilled water and then allowed to air-dry at room temperature in a dust-free environment. The nanotips were silanized by treatment with an organic cross-linking reagent, 10% GOPS in H_2O (v/v) at 90 °C for 3 h. The silanized fibers were washed with anhydrous acetonitrile and dried overnight in a vacuum oven at 105 °C. Soon after overnight incubation, the nanotips were activated by being suspended in saturated CDI in acetonitrile for 30 min followed by rinsing with acetonitrile. The silanized and activated nanotips were immersed in a solution containing DMSO, 2X reaction buffer, PBS, and LEHD-AMC and allowed to incubate for 3 h at 37 °C. The LEHD-AMC bound using this procedure remained securely immobilized during washing and subsequent manipulations in immunoassay procedures, in contrast to procedures that would use adsorption to attach proteins.^{20,21} The nanoprobes prepared were subdivided into groups to perform parallel experimental and control measurements using MCF-7 cells.

Measurement System and Procedure. Figure 3(i) shows a schematic representation of the fluorescence measurement system. The major components of this system include a HeCd laser (OmNichrome, <5 mW laser power), a Nikon Diaphot 300 inverted microscope (Nikon, Inc., Melville, NY), Hamamatsu PMT detector assembly (HC125-2), and a personal computer (PC). To perform the intracellular fluorescence measurements, the 325-nm laser line of a HeCd laser was focused onto a 600- μm delivery fiber that was terminated with a subminiature A (SMA) connector. The optical sensor was coupled to the delivery fiber through the SMA connector and secured to the microscope with micromanipulators. The fluorescence emitted from the cells was

(17) Johnson L. V, W. M. L.; Chen, L. B. *Proc. Natl. Acad. Sci U. S. A.* **1980**, *77*, 990–994.

(18) Cossarizza, A. K. G.; Grassilli, E.; Chiappelli, F.; Salviole, S.; Capri, M.; Barbieri, D.; Troiano, L.; Monti, D.; Franceschi, C. Mitochondrial modifications during rat thymocyte apoptosis: a study at the single cell level. *Exp Cell Res.* **1994**, *214*(1), 323–330.

(19) Deckwerth, T. L, J. E. M. J. Temporal analysis of events associated with programmed cell death (apoptosis) of sympathetic neurons deprived of nerve growth factor. *J. Cell Biol.* **1993**, *123*(5), 1207–1222.

(20) Sportsman, J.; Wilson, G. S. Chromatographic properties of silica-immobilized antibodies. *Anal. Chem.* **1980**, *52*(13), 2013–2018.

(21) Lin, J.; Herron, J.; Andrade, J. D. *IEEE Trans. Biomed. Eng.* **1988**, *35*, 466–471.

collected by the microscope objective and passed through a 330-nm barrier filter and then focused using the internal optics of the microscope onto the PMT for detection. The output from the PMT was recorded using a universal counter and a PC with custom-designed software for data acquisition and processing. The experimental setup used to probe single cells was adapted to this purpose from a standard micro-manipulation/microinjection apparatus. The Nikon Diaphot 300 inverted microscope, having a Diaphot 300/Diaphot 200 incubator to maintain the cell cultures at 37 °C on the microscope stage, was used for these experiments. The micromanipulation equipment consisted of MN-2 (Narishige Co. Ltd., Tokyo, Japan) Narishige three-dimensional manipulators for coarse adjustment, and Narishige MMW-23 three-dimensional hydraulic micromanipulators for fine movements. The optical sensor was mounted on a micropipet holder (World Precision Instruments, Inc., Sarasota, FL). To record the fluorescence of AMC in the evanescent field of the optical sensor, a Hamamatsu PMT detector assembly (HC125-2) was mounted in the front port of the Diaphot 300 microscope.

Before making measurements, the cells were harvested from culture flasks and transferred to culture dishes. After attachment to the bases of the Petri dishes, the experimental group of MCF-7 cells was treated with 0.5 mM ALA with subsequent photoactivation, the treated control received 0.5 mM ALA without photoactivation, while the untreated control group did not receive any treatment. For the experimental and treated control group, the solution of ALA was aspirated after a 3-h incubation period and replaced with fresh cell culture media. The experimental group of cells was then irradiated with HeNe laser to photoactivate ALA for a period of 5 min.

Using the experimental group of cells, three separate trials were conducted to determine the presence of caspase-9 activity. In addition, three separate trials were performed for the treated control and untreated control, respectively. Determination of the presence or absence of caspase-9 activity using the sensor was carried out using the following procedure. A culture dish of cells was placed on the prewarmed microscope stage set at 37 °C. The enzyme optical sensor [Figure 3(ii)], mounted on a micropipet holder of a micromanipulation system, was moved into position (i.e., in the same plane as the cells), using bright-field phase contrast microscopic illumination, so that the tip was just outside of the cell to be probed. The total magnification was 600 \times . The sensor was gently micromanipulated into the cell, past the cell membrane and extending a short way into the cytoplasm (Figure 3(iii)). During these micromanipulations, great care was taken not to penetrate the nuclear envelope and compromise the integrity of the nucleus. Room light and microscope illumination light were switched off, the laser shutter was opened, and laser light was allowed to illuminate the optical fiber and excitation light was transmitted into the fiber tip. First, a signal reading was taken with the sensor inside the cell with the laser shutter closed in order to record the dark signal. After 5 min, the laser shutter was opened allowing the excitation light to be transmitted to the nanoprobe tip and fluorescence readings were recorded. Figure 3(iii) shows an image illustrating an intracellular measurement performed in a single MCF-7 cell after micromanipulation.

In Vitro Determination of Caspase-9 Activity. We performed a calibration measurement of caspase-9 outside the cell using caspase-9 obtained from cytosolic cell extract of cell groups after apoptosis was induced and without the induction of apoptosis. This was done by inducing apoptosis in a group of cells using ALA-PDT and having a control group without ALA-PDT. The cells were harvested and the cytosolic extract placed in picofuge tubes. Optical sensors were incubated in the picofuges containing the cytosolic cell extract, one set presumably containing activated caspase-9, while the other set devoid of caspase-9.

After incubating MCF-cells using the following treatment groups, the experimental group [+]*ALA*[+]*PDT* (with ALA-PDT) and the control group [-]*ALA*[-]*PDT* (without ALA-PDT), MCF-7 cells were washed with PBS solution, pH 7.4, and then resuspended in lysis buffer

(100 mM HEPES, pH 7.4, 10% sucrose, 0.1% 3-[(3-cholamidopropyl)-dimethylammonio]-1-propanesulfonate (CHAPS), 1 mM EDTA, 10 mM dithiothreitol (DTT), 1 mM phenylmethylsulfonyl fluoride (PMSF), 10 mg/mL pepstatin, 10 mg/mL leupeptin) and left on ice for 45 min. The cells were then repeatedly passed through a syringe with a 25-gauge needle until most of the cell membrane was disrupted and centrifuged at 1500 rpm for 10 min. Activity of caspases was measured using fluorogenic substrate peptides, LEHD-AMC for caspase-9 immobilized on the nanotips of the optical sensors. The release of AMC was measured after incubating optical sensors in picofuge tubes containing the cell lysates from the various treatment groups and using a HeCd laser (excitation 325 nm) to excite AMC. Caspase activity was expressed as fluorescence intensity of AMC as a function of equivalent nanomoles of LEHD-AMC. We plotted the results of the *in vitro* measurement of caspase-9 activity. The curves for each fluorescent measurement of AMC were plotted for each as a function of nanomoles of AMC. Caspase-9 activity was determined by incubation of optical sensors with the substrate LEHD-7-amino-4-methylcoumarin (AMC) in cell lysate ($\sim 10^5$ cells) obtained from the following treatment groups, the experimental group (with ALA-PDT) and the control group (without ALA-PDT), and measured the release of AMC. The release of AMC was measured after excitation using a HeCd laser (325 nm) and collecting the fluorescence signal using a 380-nm long-pass filter. Peak emission wavelength of AMC is about 440 nm.

In Vivo Determination of Caspase-9 Activity. To perform the intracellular measurements, the optical sensor was positioned using the three-dimensional micromanipulator mounted on the inverted microscope. Using the microscope eyepiece for observation the optical sensor was micropositioned within the field of view and, once within the same plane as the cell under investigation, micromanipulated into the cytoplasm of the cell. After incubation at 37 °C for 5 min, the HeCd laser excitation source was turned on and fluorescence at λ_{max} 380 nm was measured using a 330-nm barrier filter. About 1.5–2.0 h after the induction of apoptosis, the cleavage of LEHD-AMC by caspase-9 occurs and the released AMC molecules were excited at 325 nm and the fluorescence emission was measured. The fluorescence signal emitted by AMC was collected by the fluorescence microscope optics and detected with the PMT. The fluorescence emission was collected as a function of time and the data are transmitted via a HP 53131A (225 MHz) universal counter that serves as an interface, to a PC for data acquisition and processing. Data acquisition and processing is performed using custom software built on LabView platform.

Results and Discussion

In this work, we performed a series of replicate experiments but only present a series of three mean representative acquisitions. The examination of caspase-9 activity was first performed *in vitro* using cell lysate and *in vivo*, within single MCF-7 cells, using enzyme optical sensors. Caspase-9 cleaves the substrate tetrapeptide (LEHD-AMC) between D and AMC, releasing the fluorophore AMC that is measured upon excitation by a HeCd laser. Figure 4 shows the results of *in vitro* study of the experimental group (with ALA-PDT) and the control group (without ALA-PDT). These results show a difference of about an order of magnitude in the mean fluorescence intensity measurements we obtained for the experimental group and the control group. This difference is significant enough to detect and positively identify caspase-9 activity *in vitro*. These results were expected because it is the collective effect of ALA and photoactivation that result in the induction of apoptosis and neither ALA nor photoactivation. Figure 5 (i),(ii) shows the background-subtracted results of a series of three intracellular measurements performed with enzyme optical sensors using the experimental and control group of MCF-7 cells.

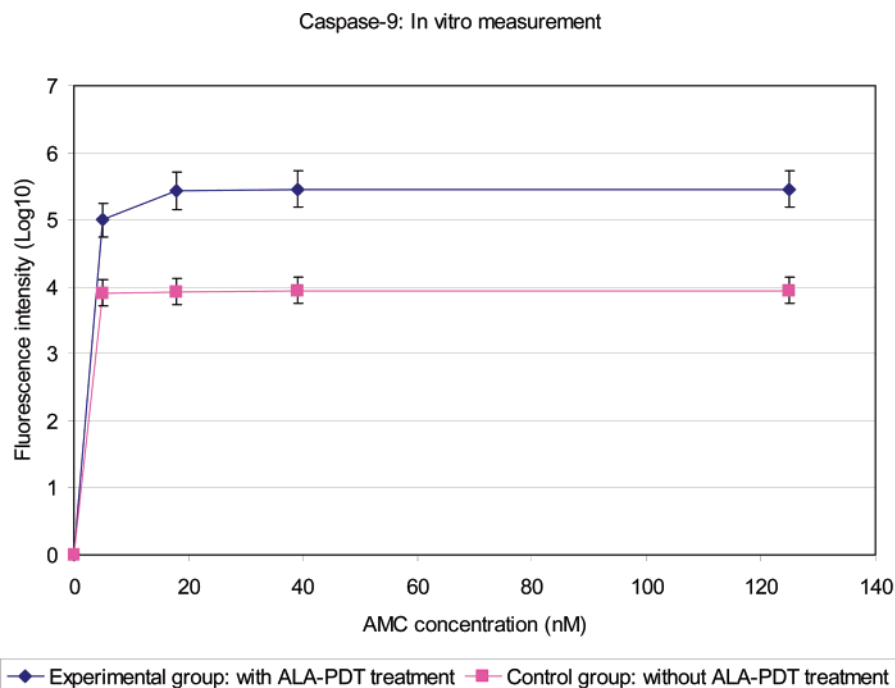


Figure 4. Graph showing the background-corrected fluorescence intensity measurements of AMC for the in vitro detection of caspase-9 activity in experimental group of MCF-7 cells, which received both ALA and photoactivation, and the control measurements for the in vitro detection of caspase-9 activity in control group of MCF-7 cells, which received neither ALA nor photoactivation. These results represent replicate studies for the measurement of caspase-9 activity with the error bars representing a 95% confidence interval (CI).

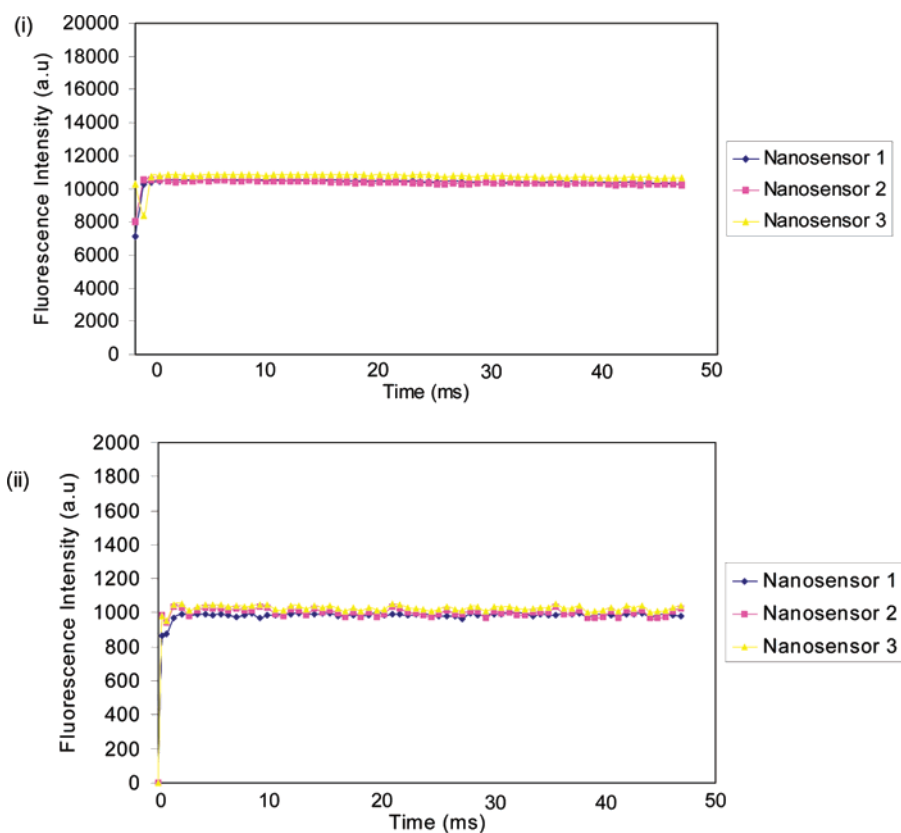


Figure 5. (i) Graph showing the background-corrected fluorescence intensity measurements of AMC for the intracellular detection of caspase-9 activity in experimental group of MCF-7 cells, which received both ALA and photoactivation. These results represent replicate studies for the measurement of caspase-9 activity. (ii) Graph showing the background-corrected control measurements for the intracellular detection of caspase-9 activity in a control group of MCF-7 cells, which received neither ALA nor photoactivation. These results represent replicate studies for the control measurement of caspase-9 activity

This graph illustrates the fluorescence intensity of AMC fluorescence as a function of time. The results show that for the control group of cells, the fluorescence signal relative to

the experimental group was not significant enough to confound the determination of AMC. Moreover, there are no other molecules that appear to interfere with the fluorescence meas-

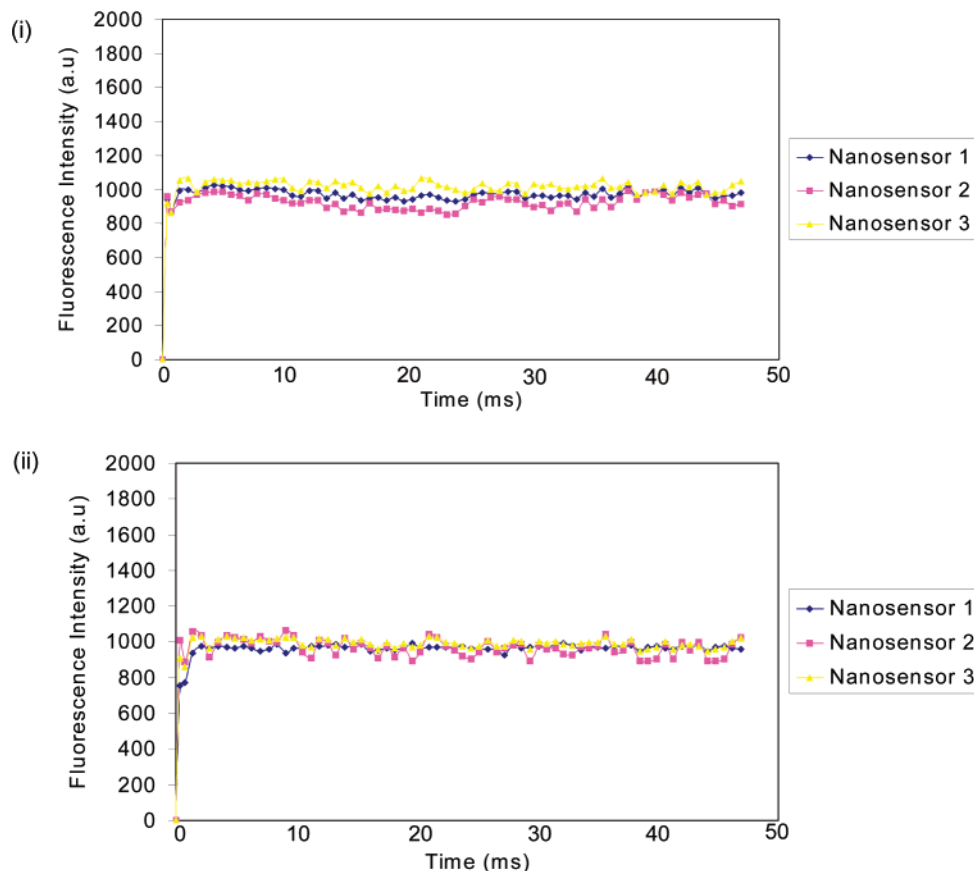


Figure 6. (i) Graph showing the background-corrected treated control measurements of the intracellular detection of caspase-9 activity in MCF-7 cells, which received ALA without photoactivation. These results represent replicate studies for the treated control measurement of caspase-9 activity within single live MCF-7 cells. (ii) Graph showing the background-corrected treated control measurements for the intracellular detection of caspase-9 activity in MCF-7 cells, which did not receive ALA but were photoactivated. These results represent replicate studies for the treated control measurement of caspase-9 activity within single live MCF-7 cells.

urements that would confound the determination of AMC due to the use of near-field excitation and detection. The application of near-field excitation contributes to the specificity of the sensor and virtually diminishes any background effects that may confound the determination of AMC because excitation of AMC occurs only in the evanescent-wave component of near-field excitation. Furthermore, the likelihood of interfering species existing within the near field is extremely small in comparison to AMC. Accordingly, the sensor used to monitor the experimental group of cells transduced a higher fluorescent signal as a result of the detection of AMC molecules momentarily sequestered at the nanotip of the optical sensor.

Figure 6 (i),(ii) shows the results of intracellular measurements performed by using the enzyme optical sensors on the treated control groups of MCF-7 cells. The first treatment group received ALA without photoactivation, while the second group received photoactivation without ALA. These graphs consist of the fluorescence intensity of AMC acquired as a function of time using three optical sensors to perform three independent measurements on MCF-7 cells. The results show that for the treated control groups, the fluorescence signal detected relative to the experimental group was not significant enough to confound the determination of AMC.

Excellent reproducibility was achieved as a result of optimization of the input parameters of the laser-based micropipet-pulling device. For instance, after determining the optimum heating temperature as well as tension applied to pull the fiber,

we successfully produced reproducible tip diameters from nanofiber to nanofiber (Figure 7 (i)). This was confirmed by acquiring several scanning electron microscope (SEM) images of the pulled fibers using a Hitachi S-4700 field emission SEM. The optimization of the input parameters of the micropipet pulling device enables very good batch-to-batch reproducibility, which is especially essential for a technology aimed to single-use sensors. For the *in vivo* studies, caspase-9 activities were analyzed in ALA-PDT treated cells (experimental group 1 in Figure 7(ii)) by measuring the fluorescence signal from AMC generated after the cleavage of the peptide substrate LEHD-AMC. Likewise, the same was done for the control groups (experimental group 2, 3, and 4 in Figure 7(ii)) of cells which received either [+]*ALA*[-]*PDT*, [-]*ALA*[+]*PDT*, or [-]*ALA*[-]*PDT*. Figure 7(ii) shows the background-subtracted results of the intracellular determination of caspase-9 activity.

The graph consists of the fluorescence intensity of AMC fluorescence as a function of illumination time. The fluorescent intensity measurements obtained for these treatment groups were then compared. As shown in Figure 7, in untreated cells, [-]*ALA*[-]*PDT*, no level of LEHD-AMC cleavage activity was detected. Likewise, the same was observed for the treated control groups, [+]*ALA*[-]*PDT* and [-]*ALA*[+]*PDT*. However, in treated cells, [+]*ALA*[+]*PDT*, significant LEHD-AMC cleavage activity via the measurement of AMC fluorescence was detected. As shown in Figure 7(ii), the initiator substrates (LEHD-AMC) of caspase-9 were cleaved into the fluorogenic AMC forms in

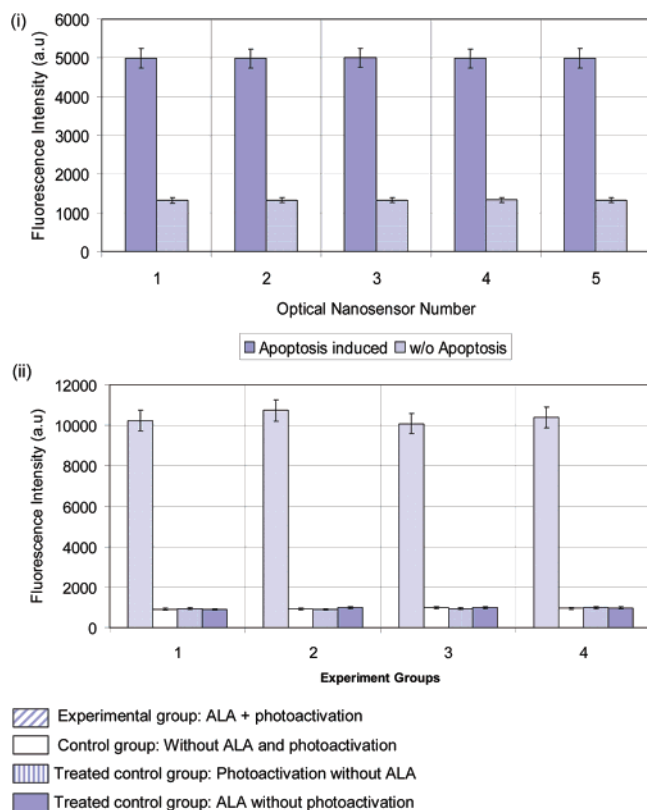


Figure 7. (i) Graph showing the reproducibility study performed using optical sensors. The calculated percent variability from optical sensor to optical sensor is within 10%. (ii) Graph showing a side-by-side comparison of caspase-9 activation in four groups of MCF-7 cells. On the X-axis, the “experiment groups” refers to the four different treatment groups, experimental group, [+]*ALA*[+]PDT, treated control group I, [+]*ALA*[−]PDT, treated control group II, [−]*ALA*[+]PDT, and the untreated control group, [−]*ALA*[−]PDT. Each bar represents an average of three intracellular measurements of caspase-9 activity in MCF-7 cells done in triplicate. The error bars shown represent a 95% confidence interval (CI). These results demonstrate the presence of active pathways of caspase-9 during *ALA*-PDT induced apoptosis in MCF-7 cells.

cells treated with *ALA*-PDT. This demonstrates the involvement of caspase-9, a member of the family of cysteine proteases that cleave after aspartic acid, in mediating apoptosis. The results obtained here demonstrated the presence of active pathways of caspase-9 during *ALA*-PDT induced apoptosis in MCF-7 cells.

The fluorescence signals obtained from the cells that were both incubated with *ALA* and photoactivated were much higher than the signal obtained from both control groups. Statistical analysis was performed on the three sets of results. The mean value of these analyses revealed that the fluorescence signal obtained using the sensors used to probe cells incubated with photoactivated *ALA* was much higher than the signal obtained by sensors used to probe untreated and treated control cell groups. A larger mean value for the experimental group affirms the detection of *AMC* and hence the detection of caspase-9 activity. The results obtained in this work demonstrate measurements performed inside single living cells using an enzyme

substrate-based optical sensor and the potential application of such a sensor in protein–protein profiling in biochemical pathways.

We have prepared enzyme substrate-based optical sensors using covalent coupling of enzyme substrate to nanotips and demonstrated the application of these sensors for the determination of the cleavage product of *LEHD-AMC*, *AMC*, in single live MCF-7 cells. The presence and detection of cleaved *AMC* in single live MCF-7 cells as a result of this design is representative of caspase-9 activity and a hallmark of apoptosis. These results indicate that *AMC*, and hence apoptosis, can be monitored and measured using optical sensors within single living cells. These results also show the possibility of cataloging cellular components, which can play an important role in understanding the role of these components and how they work together in a cell.

The studies performed in this work show the possibility of studying individual cells without having to disrupt their physiological makeup, which in the process can negatively interfere with cellular biochemistry. Mechanical and electrical manipulations such as cell lysis that can lead to cell disruption prior to the time of sampling may interfere with measurements of cellular biochemistry by initiating cellular repair mechanisms. With the optical sensors, the absence of cell manipulation prior to measurement results in virtually no effects on the cell at the time of sampling. Moreover, since many cellular signaling pathways act on time scales of a few seconds, there is critical need for single cell measurement techniques with time resolution to perform intracellular measurements. The nanoscale size optical sensor is a suitable technology that can be applied to solitary cells and has great potential for intracellular measurement of biological entities as demonstrated in this work.

In this work, an optical sensor having a nanoprobe enabled the measurement of a cellular process, in this case the functioning of an apoptosis enzyme, caspase-9, in its native environment. This work demonstrated a tool that has the potential to shed light on the principles that govern cell-signaling organization. Future work will involve studies that will attempt to carry out similar analysis on other proteins involved in biochemical cellular pathways.

Acknowledgment. This research was sponsored by the Laboratory Directed Research and Development Program (Advanced Nanosystems Project), Oak Ridge National Laboratory, by the U.S Department of Energy (DOE) Office of Chemical and Biological National Security and the DOE Office of Biological and Environmental Research, under contract DEAC05-000OR22725 with UT-Battelle, LLC. Joon Myong Song is supported by a joint appointment of the Oak Ridge National Laboratory and Oak Ridge Institute of Science Education. Paul M. Kasili is supported by the University of Tennessee-Oak Ridge National Laboratory Graduate School of Genome Science and Technology.

JA037388T